Received: 1 December 2021 | Revised: 19 January 2022 | Accepted: 7 February 2022

DOI: 10.1049/rsn2.12238

IET Radar, Sonar & Navigation

The Institution of Engineering and Technology WILEY

ORIGINAL RESEARCH

Distributed joint target detection, tracking and classification via Bernoulli filter

Gaiyou Li[1] | **Ping Wei**[1] | **Giorgio Battistelli**[2] | **Luigi Chisci**[2] | **Lin Gao**[1] | **Alfonso Farina**[3]

[1]School of Information and Communication Engineering, University of Electronic Science and Technology of China, Chengdu, Sichuan, China

[2]Dipartimento di Ingegneria dell'Informazione (DINFO), Università degli Studi di Firenze, Florence, Italy

[3]Professional Consultant, Rome, Italy

Correspondence

Luigi Chisci, Dipartimento di Ingegneria dell'Informazione (DINFO), Università degli Studi di Firenze, Florence, Italy.
Email: luigi.chisci@unifi.it

Funding information

National Natural Science Foundation of China, Grant/Award Number: 62101112

Abstract

This paper aims to solve the problem of distributed joint detection, tracking and classification (D-JDTC) of a target on a peer-to-peer sensor network. The target can be present or not, can belong to different classes, and depending on its class can behave according to different kinematic modes. Accordingly, it is modelled as a suitably extended Bernoulli random finite set (RFS) uniquely characterized by existence, classification, class-conditioned mode and class & mode-conditioned state probability distributions. Existing algorithms have been devised to perform target JDTC based on a single sensor and can only be easily extended to multiple sensors in a centralized configuration, wherein a fusion centre gathers measurements from all sensors. In this paper, by designing a suitable rule for fusing local posteriors that convey information on target existence, class, mode and state from different sensor nodes, a novel scalable and fault-tolerant D-JDTC Bernoulli filter is proposed, and its performance is evaluated by means of simulation experiments.

KEYWORDS

Bayes methods, estimation theory, sensor fusion, tracking, tracking filters

1 | INTRODUCTION

Target detection and tracking are crucial tasks in surveillance (e.g. radar [1, 2], sonar [3], autonomous driving [4] and mobile robotics [5]) systems. Though a possible approach is to separately deal with detection and tracking as two sequential phases [6], that is, by first performing target initialization followed by track maintenance, it has been recognized that joint processing of both tasks can substantially enhance the overall performance [7]. In certain circumstances, it is also desired to perform target classification for high-level applications, for example, situation assessment [8–10] and air surveillance [11]. Moreover, knowledge of the target class provides valuable information on the possible kinematic behaviours of the target [12] (e.g. a fighter aircraft can perform sharper manoeuvres than a cargo aircraft), which in turn, can be profitably exploited to improve tracking performance [13]. To this end, it is possible to perform classification based on the results of target tracking and then the class information is fed back to the tracking procedure, where the classification can be carried out, for instance, by means of the belief function theory [11]. The recent development of *random finite set* (RFS) methods has produced several interesting contributions to *joint detection, tracking and classification* (JDTC) of both single and multiple targets [14–20] but all based on a single-sensor system.

In many practical scenarios, however, multi-sensor [21] surveillance systems entail significant advantages in terms of enhanced tracking accuracy, target observability [22], reliability as well as expanded coverage [23], thus motivating the interest of the present work for multi-sensor JDTC. In the multi-sensor case, it is possible to adopt a centralized configuration, wherein a fusion centre gathers measurements from all sensors [24], or a distributed one, wherein each sensor updates a local posterior with its own measurements and then fuses it

with the posteriors of the neighbours. It is well recognized that centralized fusion can provide better performance while, on the other hand, distributed fusion is preferable in terms of scalability and fault tolerance [25].

The goal of this paper is to address single-target multi-sensor JDTC with special emphasis on the distributed configuration. In order to account for target appearance/disappearance and the presence of clutter, the target is modelled as a Bernoulli RFS [26]. Then, for classification purposes, different target classes are considered, each being characterized by a different set of possible kinematic modes. Overall, target's information, to be recursively propagated in time, consists of *existence probability* (EP), *class probability mass function* (CPMF), class-conditioned (kinematic) *mode PMFs* (MPMFs) and class&mode-conditioned *state probability density functions* (SPDFs). It is worth to point out that the joint estimation of class and mode positively affects both classification and tracking. In fact, kinematic mode information can be exploited for target classification, and inversely, class information can help to define the possible modes of a target, thus improving tracking performance [14].

In the centralized case, the optimal posterior based on measurements from all sensors can be obtained at each iteration following the Bayesian approach. In the distributed case, on the other hand, the local posterior of each sensor is first obtained with the existing Bernoulli-JDTC method [15], and then *generalized covariance intersection* (GCI) [27–30] is exploited to distributedly fuse local posteriors so as to achieve EP, CPMF, MPMFs and SPDFs of the global posterior. Furthermore, the *Gaussian mixture* (GM) implementation of the proposed method is provided.

Summarizing, the main contributions of this paper are as follows: (i) *distributed JDTC* (D-JDTC) on a peer-to-peer (i.e. without any fusion centre) sensor network is addressed; (ii) the more communication & computationally efficient GM implementation of multi-sensor JDTC is presented, as opposed to the particle filter implementation adopted in Ref. [15] for the single-sensor JDTC Bernoulli filter. Notice that, to the best of our knowledge, this is the first paper addressing distributed JDTC.

The rest of this paper is organized as follows: Section 2 formulates the multi-sensor JDTC problem considered in this paper. Sections 3 and 4 present centralized and distributed multi-sensor JDTC Bernoulli filters, respectively. Section 5 deals with the Gaussian-mixture implementation of the proposed filters. Section 6 evaluates the performance of the proposed filters by simulation experiments. Finally, Section 7 ends the paper with concluding remarks.

2 | PROBLEM FORMULATION

This section formulates the JDTC problem of interest, relative to a single target in a cluttered environment surveiled by multiple sensors. We will first model target dynamics and then multi-sensor measurement generation.

2.1 | Network model and processing procedure

This paper considers multi-sensor JDTC according to two types of configurations, referred to as *centralized* and *distributed*, schematized in Figure 1. Hereafter, $\mathcal{N}$ denotes the set of sensors of cardinality $|\mathcal{N}| = N$.

In the centralized case, each sensor $i \in \mathcal{N}$ transmits, at each time k, its measurement set $\mathcal{Z}_k^i$ to a fusion centre, wherein a centralized fusion is carried out. However, the centralized configuration is not scalable with respect to the number of sensors and has also a single point of failure (the fusion centre).

For this reason, this paper mainly focusses on the distributed setting of Figure 1b, wherein the sensor network is characterized by the following features: (1) there is no central fusion node; (2) each node only exchanges information with its neighbours. From the mathematical point of view, the network topology is described in terms of a directed graph $\mathcal{G} = (\mathcal{N}, \mathcal{E})$ where $\mathcal{E} \subseteq \mathcal{N} \times \mathcal{N}$ is the set of edges (links), such that $(i, j) \in \mathcal{E}$ if node j receives information from node i. Moreover, for each node i, $\mathcal{N}^i$ is the set of its in-neighbours (including node i itself) from which it receives information. In particular, as shown in Figure 1b, node i performs local filtering with the measurement set $\mathcal{Z}_k^i$, combines its local information with the one from the in-neighbours via GCI fusion, and provides its local information to the out-neighbours.

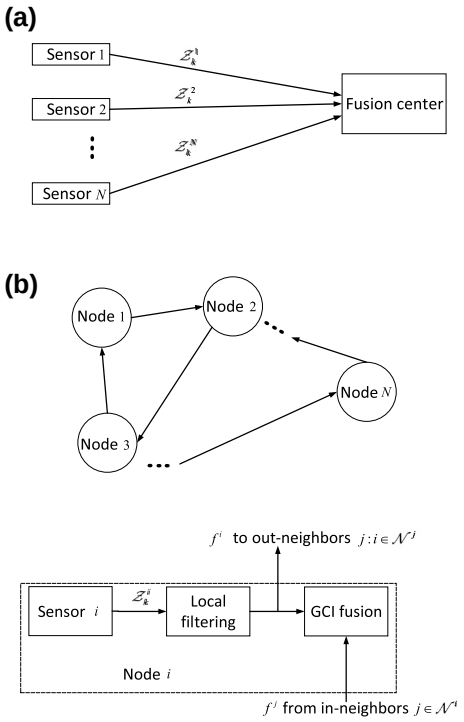

FIGURE 1 Two configurations of multi-sensor network. (a) Centralized. (b) Distributed

2.2 | Target dynamics

To represent the target, let us introduce the following three items: *kinematic state* $x \in \mathbb{X}$, $\mathbb{X}$ being an Euclidean state space; *class* $c \in \mathcal{C}$, $\mathcal{C} = \{c_1, \ldots, c_{|\mathcal{C}|}\}$ being a discrete class set; *(kinematic) mode* $m \in \mathcal{M}_c$, $\mathcal{M}_c = \{m_{c,1}, \ldots, m_{c,|\mathcal{M}_c|}\}$ being a class-dependent discrete mode set, where $|\cdot|$ denotes *cardinality*. To summarize target information, it is, therefore, convenient to define the augmented state vector $\mathbf{x} = [x^\top, c, m]^\top \in \mathbb{X} \times \mathcal{C} \times \mathcal{M}_c$.

Since the target can either exist or not, it is naturally modelled as a Bernoulli RFS, which can be either empty or a singleton, in the augmented state space, with some *existence probability* (EP) $r \in [0, 1]$. Accordingly, the target set density is defined as

$$f(\mathcal{X}) = \begin{cases} 1 - r, & \text{if } \mathcal{X} = \emptyset \\ r\, s(\mathbf{x}), & \text{if } \mathcal{X} = \{\mathbf{x}\} \\ 0, & \text{if } |\mathcal{X}| > 1 \end{cases} \tag{1}$$

where $s(\mathbf{x}) = s(x, c, m)$ is the augmented *state PDF*; by the *chain rule*, such a PDF can be factored as

$$s(\mathbf{x}) = s(x, c, m) = s(x|c, m)\, \beta(m|c)\, \gamma(c) \tag{2}$$

where $\gamma(c)$ is the *class PMF* (CPMF); $\beta(m\,|\,c)$ is the class-conditioned *mode PMF* (MPMF); $s(x\,|\,c, m)$ is the class&mode-conditioned *state PDF* (SPDF). Hence, the target is completely characterized by EP r, CPMF $\gamma(\cdot)$, MPMFs $\{\beta(\cdot|c)\}_{c\in\mathcal{C}}$ and SPDFs $\{s(\cdot|c, m)\}_{c\in\mathcal{C}, m\in\mathcal{M}_c}$. For the sake of simplicity, hereafter, the Bernoulli set density (1)–(2) will be referred to the shorthand notation $f = \{r, \gamma, \beta, s\}$.

The target dynamics has to account for appearance (birth), disappearance (death) and motion. In this respect, it can be completely characterized by the transition density $\Phi_{k|k-1}(\mathcal{X}_+|\mathcal{X})$, which expresses, in probabilistic terms, the transition of the target set from $\mathcal{X}$ at time $k-1$ to $\mathcal{X}_+$ at time k. Specifically,

$$\Phi_{k|k-1}(\mathcal{X}_+|\emptyset) = \begin{cases} 1 - p_B, & \text{if } \mathcal{X}_+ = \emptyset \\ p_B \cdot b(\mathbf{x}_+), & \text{if } \mathcal{X}_+ = \{\mathbf{x}_+\} \end{cases} \tag{3}$$

$$\Phi_{k|k-1}(\mathcal{X}_+|\{\mathbf{x}\}) = \begin{cases} 1 - p_S, & \text{if } \mathcal{X}_+ = \emptyset \\ p_S \cdot \phi_{k|k-1}(\mathbf{x}_+|\mathbf{x}), & \text{if } \mathcal{X}_+ = \{\mathbf{x}_+\} \end{cases} \tag{4}$$

where p_B and p_S are the probabilities of appearance of a newborn target and survival of an existing target, respectively; $b(\mathbf{x}_+) = \gamma_B(c_+)\, \beta_B(m_+|\,c_+)\, s_B(x_+|\,c_+, m_+)$ is the a priori state PDF of the potential new target; $\phi_{k|k-1}(\mathbf{x}_+|\,\mathbf{x})$ is the transition PDF, in the augmented state space, of the existing target. For ease of presentation, the survival probability p_S is supposed to be independent of the (augmented) state, but all the ensuing developments can be readily generalized to the case of a state-dependent survival probability. For the target class, mode and state evolution, the following reasonable assumptions are made:

- The target class remains constant over time, that is, $c_k = c_{k-1}$;
- The mode transition is governed by a class-dependent homogeneous Markov chain with transition probabilities

$$Prob(m_k = m_+|m_{k-1} = m, c) = \pi_c(m_+|m); \tag{5}$$

- The target motion is modelled by the mode-dependent state transition density

$$Prob(x_k = x_+|x_{k-1} = x, m_k = m) = \varphi(x_+|x, m). \tag{6}$$

Taking into account the above assumptions, the transition PDF turns out to be,

$$\begin{aligned} \Phi_{k|k-1}(\mathbf{x}_+|\mathbf{x}) &= \Phi_{k|k-1}(x_+, c_+, m_+|x, c, m) \\ &= \delta_{c_+,c}\, \pi_c(m_+|m)\, \varphi(x_+|x, m_+) \end{aligned} \tag{7}$$

where $\delta_{c_+,c}$ is the *Kronecker delta* equal to 1 if $c_+ = c$ and to zero otherwise.

2.3 | Multi-sensor measurement model

The area of interest is monitored by a set of sensors $\mathcal{N}$. At sampling time k, sensor node $i \in \mathcal{N}$ provides the measurement RFS

$$\mathcal{Z}_k^i = \mathcal{T}^i(\mathcal{X}_k) \cup \mathcal{K}_k^i, \tag{8}$$

which is the union of the target-originated RFS $\mathcal{T}^i(\mathcal{X}_k)$ and the clutter set $\mathcal{K}_k^i$. The target-originated RFS takes the form,

$$\begin{aligned} \mathcal{T}^i(\mathcal{X}_k) &= \begin{cases} \emptyset, & \text{if } \mathcal{X}_k = \emptyset \\ \emptyset, & \text{if } \mathcal{X}_k = \{\mathbf{x}_k\} \text{ with prob. } 1 - p_D^i(x_k, c) \\ z_k^i, & \text{if } \mathcal{X}_k = \{\mathbf{x}_k\} \text{ with prob. } p_D^i(x_k, c) \end{cases} \\ z_k^i &\sim \ell^i(z_k^i|x_k) \end{aligned} \tag{9}$$

where $\ell^i(z\,|\,x)$ is the likelihood function associated to the *ith* sensor. The clutter set $\mathcal{K}_k^i$ is modelled as Poisson RFS [31] with *probability hypothesis density* (PHD) $\kappa(z)$ defined over the measurement space. The measurements of different sensors are supposed to be mutually conditionally independent. Notice

that, in the considered multi-sensor measurement model, the target class $c \in \mathcal{C}$ only affects detection probabilities $p_D^i(x,c)$ while the target mode $m \in \mathcal{M}_c$ is irrelevant.

3 | CENTRALIZED JDTC-BF ALGORITHM

This section focusses on the centralized configuration, wherein all sensor nodes $i \in \mathcal{N}$ convey their measurement sets $\mathcal{Z}_k^i$ to a fusion centre that, in principle, should be able to perform optimal multi-sensor fusion, that is, to provide the Bernoulli set density $f\left(\mathcal{X}_k | \bigcup_{i\in\mathcal{N}} \mathcal{Z}_{1:k}^i\right)$ where $\mathcal{Z}_{1:k}^i$ denotes the sequence of measurements collected by sensor i from time 1 to time k. Hereafter, it will be shown how to extend the joint detection and tracking Bernoulli filtering approach of Ref. [7,25,31] to the JDTC setting of this paper. Specifically, assuming that at time $k-1$, the augmented Bernoulli density $f_{k-1} = \{r_{k-1}, \gamma_{k-1}, \beta_{k-1}, s_{k-1}\}$ is given and following a Bayesian approach, the aim is to first perform prediction to obtain $f_{k|k-1} = \{r_{k|k-1}, \gamma_{k|k-1}, \beta_{k|k-1}, s_{k|k-1}\}$ by exploiting the target dynamics (3)-(7) and then followed by multi-sensor update to get $f_k = \{r_k, \gamma_k, \beta_k, s_k\}$ by exploiting the measurement model (8).

3.1 | JDTC-BF prediction

Prediction of a standard Bernoulli RFS density $f_{k-1} = \{r_{k-1}, s_{k-1}\}$ into $f_{k|k-1} = \{r_{k|k-1}, s_{k|k-1}\}$ can be found in Ref. [25] and Equations (10)–(12). The following result [15] provides the extension of such prediction to a Bernoulli RFS density defined over the augmented class-mode-state space.

Proposition 1. *Ref. [15] Given the Bernoulli RFS density $f_{k-1} = \{r_{k-1}, \gamma_{k-1}, \beta_{k-1}, s_{k-1}\}$, the predicted density $f_{k|k-1} = \{r_{k|k-1}, \gamma_{k|k-1}, \beta_{k|k-1}, s_{k|k-1}\}$ is obtained as follows:*

$$r_{k|k-1} = p_B(1-r_{k-1}) + p_S\, r_{k-1}, \tag{10}$$

$$\gamma_{k|k-1}(c) = \frac{p_B(1-r_{k-1})}{r_{k|k-1}}\gamma_B(c) + \frac{p_S\, r_{k-1}}{r_{k|k-1}}\gamma_{k-1}(c), \tag{11}$$

$$\begin{aligned}\beta_{k|k-1}(m|c) = {} & \frac{p_B(1-r_{k-1})}{r_{k|k-1}\gamma_{k|k-1}(c)}\gamma_B(c)\beta_B(m|c) \\ & + \frac{p_S\, r_{k-1}}{r_{k|k-1}\gamma_{k|k-1}(c)}\gamma_{k-1}(c) \\ & \times \sum_{m'\in\mathcal{M}_c} \pi_c(m|m')\beta_{k-1}(m'|c),\end{aligned} \tag{12}$$

$$\begin{aligned}s_{k|k-1}(x|c,m) = {} & \frac{p_B(1-r_{k-1})\,\gamma_B(c)}{r_{k|k-1}\gamma_{k|k-1}(c)\beta_{k|k-1}(m|c)} \\ & \times \beta_B(m|c)\, s_B(x|c,m) \\ & + \frac{p_S\, r_{k-1}\gamma_{k-1}(c)}{r_{k|k-1}\gamma_{k|k-1}(c)\beta_{k|k-1}(m|c)} \\ & \times \sum_{m'\in\mathcal{M}_c} \pi_c(m|m')\beta_{k-1}(m'|c) \\ & \times \int \varphi(x|x',m)\, s_{k-1}(x'|c,m')dx'.\end{aligned} \tag{13}$$

3.2 | JDTC-BF centralized multi-sensor update

The following result extends in a straightforward way the single-sensor update in Ref. [15] to the centralized multi-sensor update of the augmented target Bernoulli density.

Proposition 2. *Given the predicted Bernoulli RFS density $f_{k|k-1} = \{r_{k|k-1}, \gamma_{k|k-1}, \beta_{k|k-1}, s_{k|k-1}\}$ and the measurement RFSs $\left\{\mathcal{Z}_k^i\right\}_{i\in\mathcal{N}}$, the updated density $f_k = \{r_k, \gamma_k, \beta_k, s_k\}$ is obtained as follows:*

$$r_k = \frac{r_{k|k-1}\sum_{c\in\mathcal{C}}\gamma_{k|k-1}(c)\,\ell(c)}{1 - r_{k|k-1} + r_{k|k-1}\sum_{c\in\mathcal{C}}\gamma_{k|k-1}(c)\,\ell(c)}, \tag{14}$$

$$\gamma_k(c) = \frac{\gamma_{k|k-1}(c)\;\ell(c)}{\sum_{c\in\mathcal{C}}\gamma_{k|k-1}(c)\,\ell(c)}, \tag{15}$$

$$\beta_k(m|c) = \frac{\beta_{k|k-1}(m|c)\,\ell(m|c)}{\sum_{m\in\mathcal{M}_c}\beta_{k|k-1}(m|c)\,\ell(m|c)}, \tag{16}$$

$$s_k(x|c,m) = \frac{s_{k|k-1}(x|c,m)\,\ell(x|c,m)}{\int s_{k|k-1}(x'|c,m)\,\ell(x'|c,m)\,dx'}, \tag{17}$$

where

$$\ell(c) = \sum_{m\in\mathcal{M}_c}\beta_{k|k-1}(m|c)\,\ell(m|c), \tag{18}$$

$$\ell(m|c) = \int s_{k|k-1}(x|c,m)\,\ell(x|c,m)\,dx, \tag{19}$$

$$\ell(x|c,m) = \prod_{i\in\mathcal{N}}\left[1 - p_D^i(c) + p_D^i(c)\sum_{z\in\mathcal{Z}_k^i}\frac{\ell^i(z|x)}{\kappa(z)}\right]. \tag{20}$$

According to the above Propositions 1 and 2, the resulting C-JDTC-BF algorithm is given in Algorithm 1, where the maximum a posteriori probability (MAP) criterion is used for class and mode estimation, whereas the kinematic state estimate can be computed according to either the MAP or minimum mean square error (MMSE) criterion.

Algorithm 1: C-JDTC-BF (Time k)

Input: $\mathcal{Z}_k = \{\mathcal{Z}_k^i\}_{i\in\mathcal{N}}, f_{k-1} = \{r_{k-1}, \gamma_{k-1}, \beta_{k-1}, s_{k-1}\}$
Output: $f_k = \{r_k, \gamma_k, \beta_k, s_k\}$ and $\hat{\mathbf{x}}_k$
Predicted EP $r_{k|k-1}$, CPMF $\gamma_{k|k-1}(c)$, MPMFs $\beta_{k|k-1}(m|c)$ and SPDFs $s_{k|k-1}(x|m,c)$ are computed by (10)-(13);
Updated EP r_k, CPMF $\gamma_k(c)$, MPMFs $\beta_k(m|c)$ and SPDFs $s_k(x|c,m)$ are computed by (14)-(20);
if $r_k < 0.5$ **then**
    no target is detected;
else
    $\hat{c}_k = \arg\max_{c\in\mathcal{C}} \gamma_k(c)$;
    $\hat{m}_k = \arg\max_{m\in\mathcal{M}_{\hat{c}_k}} \beta_k^i(m|\hat{c}_k)$;
    Extract $\hat{x}_k$ from $s_k(\cdot|\hat{c}_k, \hat{m}_k)$ according to either MAP or MMSE criterion;
    Set $\hat{\mathbf{x}}_k = \left[(\hat{x}_k)^T, \hat{c}_k, \hat{m}_k\right]^T$;
end

4 | DISTRIBUTED JDTC-BF ALGORITHM

This section deals with the distributed setting, wherein each sensor node $i \in \mathcal{N}$ computes a local posterior $f^i = \{r^i, \gamma^i, \beta^i, s^i\}$ and fuses it with those of the in-neighbours. The idea is to approximate the global posterior $f\left(\mathcal{X}_k | \bigcup_{i\in\mathcal{N}} \mathcal{Z}_{1:k}^i\right)$ in each node via repeated fusion (consensus) iterations with the neighbouring nodes. In particular, the GCI fusion rule [32] is adopted by which the fused density is nothing but the geometrical average [33] of the fusing ones, that is,

$$\overline{f}(\mathcal{X}) = \frac{\prod_{i\in\mathcal{N}} \left[f^i(\mathcal{X})\right]^{\omega^i}}{\int \prod_{i\in\mathcal{N}} \left[f^i(\mathcal{X})\right]^{\omega^i} d\mathcal{X}}, \tag{21}$$

with suitably chosen fusion weights $\omega^i \in (0, 1)$ such that $\sum_{i\in\mathcal{N}} \omega^i = 1$. The GCI fusion of Bernoulli RFS densities $f^i = \{r^i, s^i\}$ into $\overline{f} = \{\overline{r}, \overline{s}\}$ can be found in Ref. [26] and Equations (24) and (25). The next result provides an extension to the JDTC case with augmented Bernoulli RFS densities consisting of EP, CPMF, MPMFs and SPDFs

Theorem 1. *Given local Bernoulli RFS densities $f^i = \{r^i, \gamma^i, \beta^i, s^i\}$ and fusion weights ω^i for any $i \in \mathcal{N}$, the GCI-fused density in* (21) *turns out to be a Bernoulli RFS density $\overline{f} = \{\overline{r}, \overline{\beta}, \overline{\gamma}, \overline{s}\}$ given by*

$$\overline{r} = \frac{\tilde{r}\sum_{c\in\mathcal{C}} \tilde{\gamma}(c) \sum_{m\in\mathcal{M}_c} \tilde{\beta}(m|c) \int \tilde{s}(x|c,m)dx}{\tilde{\zeta} + \tilde{r}\sum_{c\in\mathcal{C}} \tilde{\gamma}(c) \sum_{m\in\mathcal{M}_c} \tilde{\beta}(m|c) \int \tilde{s}(x|c,m)dx}, \tag{22}$$

$$\overline{\gamma}(c) = \frac{\tilde{\gamma}(c) \sum_{m\in\mathcal{M}_c} \tilde{\beta}(m|c) \int \tilde{s}(x|c,m)dx}{\sum_{c\in\mathcal{C}} \tilde{\gamma}(c) \sum_{m\in\mathcal{M}_c} \tilde{\beta}(m|c) \int \tilde{s}(x|c,m)dx}, \tag{23}$$

$$\overline{\beta}(m|c) = \frac{\tilde{\beta}(m|c) \int \tilde{s}(x|c,m)dx}{\sum_{m\in\mathcal{M}_c} \tilde{\beta}(m|c) \int \tilde{s}(x|c,m)dx}, \tag{24}$$

$$\overline{s}(x|c,m) = \frac{\tilde{s}(x|c,m)}{\int \tilde{s}(x|c,m)\,dx}, \tag{25}$$

with

$$\tilde{s}(x|c,m) = \prod_{i\in\mathcal{N}} \left[s^i(x|c,m)\right]^{\omega^i}, \tag{26}$$

$$\tilde{\beta}(m|c) = \prod_{i\in\mathcal{N}} \left[\beta^i(m|c)\right]^{\omega^i}, \tag{27}$$

$$\tilde{\gamma}(c) = \prod_{i\in\mathcal{N}} \left[\gamma^i(c)\right]^{\omega^i}, \tag{28}$$

$$\tilde{\zeta} = \prod_{i\in\mathcal{N}} \left(1 - r^i\right)^{\omega^i}, \tag{29}$$

$$\tilde{r} = \prod_{i\in\mathcal{N}} \left(r^i\right)^{\omega^i}. \tag{30}$$

Proof: see Appendix.

For the sake of scalability, the global fusion (21) over the whole network $\mathcal{N}$ is actually replaced by a sequence of $L \geq 1$ fusion (consensus) steps over the subnetwork $\mathcal{N}^i$ containing node i and its in-neighbours, that is, all nodes $j \neq i$ from which node i has received data. More precisely, for $l = 1, \cdots, L$, Equation (21) is replaced by the following iterative consensus procedure carried out in each node i:

$$f_l^i(\mathcal{X}) = \frac{\prod_{j\in\mathcal{N}^i} \left[f_{l-1}^j(\mathcal{X})\right]^{\omega^{i,j}}}{\int \prod_{j\in\mathcal{N}^i} \left[f_{l-1}^j(\mathcal{X})\right]^{\omega^{i,j}} d\mathcal{X}} \tag{31}$$

initialized from $f_0^i(\mathcal{X}) = f^i(\mathcal{X})$ and with consensus weights $\omega^{i,j} > 0$, satisfying $\sum_{j\in\mathcal{N}^i} \omega^{i,j} = 1$, possibly selected so as to ensure that $f_l^i(\mathcal{X})$ converges to $\overline{f}(\mathcal{X})$ as $l \to \infty$. The resulting D-JDTC-BF algorithm is summarized in Algorithm 2.

Algorithm 2: D-JDTC-BF (Node i, Time k)

Input: $\mathcal{Z}_k^i, f_{k-1}^i = \{r_{k-1}^i, \gamma_{k-1}^i, \beta_{k-1}^i, s_{k-1}^i\}$
Output: $f_k^i = \{r_k^i, \gamma_k^i, \beta_k^i, s_k^i\}$ and $\hat{\mathbf{x}}_k^i$

Carry out local filtering with prediction and update steps of JDTC-BF to get the local Bernoulli density $f_{k,0}^i = \{r_{k,0}^i, \gamma_{k,0}^i, \beta_{k,0}^i, s_{k,0}^i\}$;
for $l = 1, \cdots, L$ **do**
  Receive data from in-neighbors $j \in \mathcal{N}^i \backslash \{i\}$ to get $f_{k,l-1}^j = \{r_{k,l-1}^j, \gamma_{k,l-1}^j, \beta_{k,l-1}^j, s_{k,l-1}^j\}$;
  Fuse $\{f_{k,l-1}^j\}_{j\in\mathcal{N}^i}$ with weights $\omega^{i,j}$ via (22)-(30) to get $f_{k,l}^j = \{r_{k,l}^j, \gamma_{k,l}^j, \beta_{k,l}^j, s_{k,l}^j\}$;
end
Set $f_k^i = \{r_k^i, \gamma_k^i, \beta_k^i, s_k^i\} = \{r_{k,L}^i, \gamma_{k,L}^i, \beta_{k,L}^i, s_{k,L}^i\}$;
if $r_k < 0.5$ **then**
  no target is detected;
else
  $\hat{c}_k^i = \arg\max_{c\in\mathcal{C}} \gamma_k^i(c)$;
  $\hat{m}_k^i = \arg\max_{m\in\mathcal{M}_{\hat{c}_k^i}} \beta_k^i(m|\hat{c}_k^i)$;
  Extract $\hat{x}_k^i$ from $s_k^i(\cdot|\hat{c}_k^i, \hat{m}_k^i)$ according to either MAP or MMSE criterion ;
  Set $\hat{\mathbf{x}}_k^i = \left[(\hat{x}_k^i)^T, \hat{c}_k^i, \hat{m}_k^i\right]^T$;
end

Remark 1 It is worth pointing out that the D-JDTC-BF approach of this section significantly extends the previous work in Ref. [34] on distributed multiple-model Bayesian tracking of a manoeuvring target. In fact, the D-JDTC-*BF* also allows to perform target detection and classification, besides tracking, and considers the presence of clutter as well as target appearance/disappearance.

5 | GAUSSIAN-MIXTURE IMPLEMENTATION OF JDTC-BF

In this section, the JDTC-BF is implemented by utilizing the GM approach [35]. For the subsequent developments, the target motion is modelled by a mode-dependent state equation of the form,

$$\begin{aligned} x_k &= f(x_{k-1}, m_k) + w_k \\ w_k &\sim \mathcal{G}(\cdot; 0, Q(m_k)) \end{aligned} \tag{32}$$

where w_k is a Gaussian process noise with zero mean and mode-dependent covariance $Q(m_k)$. Accordingly, the kinematic state transition density is

$$\varphi(x_+|x, m_+) = \mathcal{G}(x_+; f(x, m_+), Q(m_+)). \tag{33}$$

Further, each sensor i is modelled by a measurement equation of the form,

$$\begin{aligned} z_k^i &= h^i(x_k) + v_k^i \\ v_k^i &\sim \mathcal{G}(\cdot; 0, R^i) \end{aligned} \tag{34}$$

where v_k^i is a Gaussian measurement noise with zero mean and covariance R^i. The measurement noises v_k^i of different sensors are assumed mutually independent and independent of the process noise w_k. Accordingly, the likelihood function associated with the *ith* sensor measurement model in Equation (9) is given by

$$\ell^i(z|x) = \mathcal{G}\left(z; h^i(x), R^i\right). \tag{35}$$

Hereafter, in order to approximate the likelihood function of non-linear measurement (34), we follow the EKF approach and linearize the function h^i based on the Taylor expansion at x_0

$$h^i(x) \cong h^i(x_0) + H^i(x_0)(x - x_0), \tag{36}$$

where H^i is the Jacobian matrix. Similarly, the function f is linearized as

$$f(x, m) \cong f(x_0, m) + F(x_0, m)(x - x_0) \tag{37}$$

where $F(x_0, m)$ is the Jacobian matrix with respect to x for a given m.

In the proposed implementation scheme, the GM is utilized to approximately represent SPDFs of the Bernoulli density. In particular, for a Bernoulli density $f = \{r, \gamma, \beta, s\}$, a GM with $J(c, m)$ *Gaussian components* (GCs) is employed for the SPDF

$$s(x|c, m) = \sum_{j=1}^{J(c,m)} \alpha_j(c, m) \cdot \mathcal{G}\left(x; \mu_j(c, m), P_j(c, m)\right), \tag{38}$$

where $\alpha_j(c, m)$, $\mu_j(c, m)$ and $P_j(c, m)$ are the weight, mean and covariance of jth GC conditioned on the class $c \in \mathcal{C}$ and mode $m \in \mathcal{M}_c$. Thus, the SPDF can be more compactly rewritten as $s = \left\{\alpha_j, \mu_j, P_j\right\}_{j=1}^{J(c,m)}$.

5.1 | Prediction

At time $k-1$, given the prior augmented Bernoulli density $f_{k-1} = \{r_{k-1}, \gamma_{k-1}, \beta_{k-1}, s_{k-1}\}$ with class&mode-conditioned SPDFs represented in GM form,

$$\begin{aligned} s_{k-1}(x|c, m) &= \sum_{j=1}^{J_{k-1}(c,m)} \alpha_{k-1,j}(c, m) \\ &\quad \times \mathcal{G}\left(x; \mu_{k-1,j}(c, m), P_{k-1,j}(c, m)\right) \end{aligned} \tag{39}$$

and the augmented birth Bernoulli density $f_B = \{p_B, \gamma_B, \beta_B, s_B\}$ with SPDFs represented in GM form,

$$s_B(x|c,m) = \sum_{j=1}^{J_B(c,m)} \alpha_{B,j}(c,m)\mathcal{G}\Big(x;\mu_{B,j}(c,m),P_{B,j}(c,m)\Big),$$

then the class&mode-conditioned SPDF of the augmented predicted density $f_{k|k-1} = \{r_{k|k-1}, \beta_{k|k-1}, \gamma_{k|k-1}, s_{k|k-1}\}$ via Equations (10)–(13) is given by

$$\begin{aligned} s_{k|k-1}(x|c,m) = &\frac{p_B(1-r_{k-1})\gamma_B(c)\beta_B(m|c)}{r_{k|k-1}\gamma_{k|k-1}(c)\beta_{k|k-1}(m|c)} \\ &\times \sum_{j=1}^{J_B(c,m)} \alpha_{B,j}(c,m) \\ &\times \mathcal{G}\Big(x;\mu_{B,j}(c,m),P_{B,j}(c,m)\Big) \\ &+ \frac{p_S r_{k-1}\gamma_{k-1}(c)}{r_{k|k-1}\gamma_{k|k-1}(c)\beta_{k|k-1}(m|c)} \\ &\times \sum_{m'\in\mathcal{M}_c} \pi_c(m|m')\beta_{k-1}(m'|c) \\ &\times \sum_{j=1}^{J_{k-1}(c,m')} \alpha_{k-1,j}(c,m') \\ &\times \mathcal{G}\Big(x;\mu^S_{k|k-1,j}(c,m,m'),P^S_{k|k-1,j}(c,m,m')\Big), \end{aligned} \tag{40}$$

where

$$\mu^S_{k|k-1,j}(c,m,m') = f\Big(\mu_{k-1,j}(c,m'),m\Big) \tag{41}$$

$$P^S_{k|k-1,j}(c,m,m') = F_{k,j}P_{k-1,j}(c,m')F^\top_{k,j} + Q_k(m) \tag{42}$$

$$F_{k,j} = \frac{\partial f}{\partial x}\Big(\mu_{k-1,j}(c,m'),m\Big). \tag{43}$$

Notice that the predicted densities $s_{k|k-1}(x|c,m)$ in Equation (40) are still in GM form, but with an increased number of GCs given by

$$J_{k|k-1}(c,m) = J_B(c,m) + \sum_{m'\in\mathcal{M}_c} J_{k-1}(c,m'), \tag{44}$$

and can, therefore, be rearranged as

$$\begin{aligned} s_{k|k-1}(x|c,m) = &\sum_{j=1}^{J_{k|k-1}(c,m)} \alpha_{k|k-1,j}(c,m) \\ &\times \mathcal{G}\Big(x;\mu_{k|k-1,j}(c,m),P_{k|k-1,j}(c,m)\Big) \end{aligned} \tag{45}$$

for appropriate weights, means and covariances of the GCs.

5.2 | Single-sensor update of local JDTC-BF

Let us now consider a single-sensor update with the local measurement set $\mathcal{Z}_k = \mathcal{Z}^i_k$, omitting for the sake of simplicity superscript i. Starting from the predicted density $f_{k|k-1} = \{r_{k|k-1}, \gamma_{k|k-1}, \beta_{k|k-1}, s_{k|k-1}\}$, we can, therefore, apply Equations (14)–(17) to get $f_k = \{r_k, \gamma_k, \beta_k, s_k\}$. Exploiting the GM form Equation (45) of $s_{k|k-1}(x|c,m)$ and Equation (35), the likelihoods Equation (19) take the form,

$$\begin{aligned} \ell(m|c) = &[1-p_D(x,c)] \\ &+ p_D(x,c)\sum_{z\in\mathcal{Z}_k}\sum_{j=1}^{J_{k|k-1}(c,m)} \alpha_{k,j}(c,m,z). \end{aligned} \tag{46}$$

Accordingly, the updated SPDFs in Equation (17) become as follows:

$$\begin{aligned} s_k(x|c,m) = \frac{1}{\Lambda}\times\Bigg[&[1-p_D(x,c)]\sum_{j=1}^{J_{k|k-1}(c,m)} \alpha_{k|k-1,j}(c,m) \\ &\times \mathcal{G}\Big(x;\mu_{k|k-1,j}(c,m),P_{k|k-1,j}(c,m)\Big) \\ &+ p_D(c)\sum_{z\in\mathcal{Z}_k}\sum_{j=1}^{J_{k|k-1}(c,m)} \alpha_{k,j}(c,m,z) \\ &\times \mathcal{G}\Big(x;\mu_{k,j}(c,m,z),P_{k,j}(c,m)\Big)\Bigg] \end{aligned} \tag{47}$$

$$\begin{aligned} \Lambda = &[1-p_D(c)] \\ &+ p_D(c)\sum_{z\in\mathcal{Z}_k}\sum_{j=1}^{J_{k|k-1}(c,m)}\alpha_{k,j}(c,m,z) \end{aligned} \tag{48}$$

$$\alpha_{k,j}(c,m,z) = \frac{q(z)}{\kappa(z)}\alpha_{k|k-1,j}(c,m) \tag{49}$$

$$q(z) = \mathcal{G}\Big(z;h\Big(\mu_{k|k-1,j}(c,m)\Big),S_{k,j}\Big) \tag{50}$$

$$\begin{aligned} \mu_{k,j}(c,m,z) = &\mu_{k|k-1,j}(c,m) \\ &+ K_{k,j}\Big(z - h\Big(\mu_{k|k-1,j}(c,m)\Big)\Big) \end{aligned} \tag{51}$$

$$H_{k,j} = \frac{\partial h}{\partial x}\Big(\mu_{k|k-1,j}(c,m)\Big) \tag{52}$$

$$P_{k,j}(c,m) = \big(I - K_{k,j}H_{k,j}\big)P_{k|k-1,j}(c,m) \tag{53}$$

$$K_{k,j} = P_{k|k-1,j}(c,m)H^\top_{k,j}S^{-1}_{k,j} \tag{54}$$

$$S_{k,j} = R + H_{k,j} P_{k|k-1,j}(c,m) H_{k,j}^{\mathsf{T}}. \tag{55}$$

Notice that Equation (47) is in GM form, as required for the subsequent steps, with a number of GCs,

$$J_k(c,m) = (|\mathcal{Z}_k| + 1) J_{k|k-1}(c,m) \tag{56}$$

increased by a factor equal to the number of measurement plus one.

Remark 2 JDTC aims to jointly estimate target state, class and mode. In Ref. [15], the proposed method solves the problem by exploiting a sequential Monte Carlo (SMC) implementation of the Bernoulli filter. Since typically GM representation of a PDF is more parsimonious than SMC representation and also because JDTC involves multiple SPDFs for all class-mode pairs (c, m), the GM approach seems by far preferable, especially in the distributed case, wherein posteriors are transmitted and received by each sensor node. Unfortunately, however, the number of GCs increases at each Bayesian step (prediction, update or fusion) so that suitable pruning and/or merging procedures (see Ref. [36], Table II]) are needed to limit such a number.

5.3 | Multi-sensor update of C-JDTC-BF

Proposition 2 provides the update equations based on the Bayes-optimal C-JDTC-BF. In the multi-sensor case, for the class&mode-conditioned SPDF, it is possible to implement centralized fusion by iterating single-sensor Bernoulli filter updates as follows [15]:

- Starting from the prior $s_k^{(0)} = s_{k|k-1}$, first compute $s_k^{(1)} = \left\{\alpha_{k,j}^{(1)}, \mu_{j,k}^{(1)}, P_{k,j}^{(1)}\right\}_{j=1}^{J_k^{(1)}(c,m)}$ using measurements and parameters of sensor 1 according to the single-sensor Bernoulli filter update procedure of the previous subsection
- Next, apply the same procedure to the prior $s_k^{(1)}$, with measurements and parameters of sensor 2, to get $s_k^{(2)} = \left\{\alpha_{k,j}^{(2)}, \mu_{k,j}^{(2)}, P_{k,j}^{(2)}\right\}_{j=1}^{J_k^{(2)}(c,m)}$
- Repeat the same step until all sensors have been considered and $s_k = s_k^{(|\mathcal{N}|)}$ is obtained

The multi-sensor updated Bernoulli density $f_k = \{r_k, \gamma_k, \beta_k, s_k\}$ can be obtained by using Equations (14)–(17). Furthermore, the updated SPDFs in Equation (17) are computed by using the above-mentioned iterations

$$s_k(x|c,m) = \Psi_k^{(|\mathcal{N}|)} \circ \cdots \circ \Psi_k^{(2)} \circ \Psi_k^{(1)}\left[s_{k|k-1}(x|c,m)\right] \tag{57}$$

where $\circ$ denotes composition, and

$$\begin{aligned}
\Psi_k^{(i)}\left[s_k^{(i-1)}(x|c,m)\right] &= \frac{1}{\Lambda^{(i)}} \times \left[\left[1 - p_D^{(i)}(c)\right]\right. \\
&\quad \times \sum_{j=1}^{J_k^{(i-1)}(c,m)} \tilde{\alpha}_{k,j}^{(i-1)}(c,m) \\
&\quad \times \mathcal{G}\left(x; \tilde{\mu}_{k,j}^{(i-1)}(c,m), \tilde{P}_{k,j}^{(i-1)}(c,m)\right) \\
&\quad + p_D^{(i)}(c) \sum_{z \in \mathcal{Z}_k^i} \sum_{j=1}^{J_k^{(i-1)}(c,m)} \alpha_{k,j}^{(i)}(c,m,z) \\
&\quad \left. \times \mathcal{G}\left(x; \mu_{k,j}^{(i)}(c,m,z), P_{k,j}^{(i)}(c,m)\right)\right] \\
&= \frac{1}{\Lambda^{(i)}} \left[\sum_{j=1}^{J_k^{(i)}(c,m)} \tilde{\alpha}_{k,j}^{(i)}(c,m) \right. \\
&\quad \left. \times \mathcal{G}\left(x; \tilde{\mu}_{k,j}^{(i)}(c,m), \tilde{P}_{k,j}^{(i)}(c,m)\right)\right]
\end{aligned} \tag{58}$$

where $\tilde{\alpha}_{k,j}^{(0)}(c,m) = \alpha_{k|k-1,j}(c,m)$ $\tilde{\mu}_{k,j}^{(0)}(c,m) = \mu_{k|k-1,j}(c,m)$ $\tilde{P}_{k,j}^{(0)}(c,m) = P_{k|k-1,j}(c,m)$, and

$$\begin{aligned}
\Lambda^{(i)} &= \left[1 - p_D^{(i)}(c)\right] \\
&\quad + p_D^i(c) \sum_{z \in \mathcal{Z}_k^{(i)}} \sum_{j=1}^{J_k^{(i-1)}(c,m)} \alpha_{k,j}^{(i)}(c,m,z)
\end{aligned} \tag{59}$$

$$J_k^{(i)}(c,m) = J_k^{(i-1)}(c,m) + |\mathcal{Z}_k^i| J_k^{(i-1)}(c,m) \tag{60}$$

$$\alpha_{k,j}^{(i)}(c,m,z) = \frac{q^{(i)}(z)}{\kappa(z)} \tilde{\alpha}_{k,j}^{(i-1)}(c,m) \tag{61}$$

$$q^{(i)}(z) = \mathcal{G}\left(z; h\left(\tilde{\mu}_{k,j}^{(i-1)}(c,m)\right), S_{k,j}^{(i)}\right) \tag{62}$$

$$\begin{aligned}
\mu_{k,j}^{(i)}(c,m,z) &= \tilde{\mu}_{k,j}^{(i-1)}(c,m) \\
&\quad + K_{k,j}^{(i)}\left(z - h\left(\tilde{\mu}_{k,j}^{(i-1)}(c,m)\right)\right)
\end{aligned} \tag{63}$$

$$H_{k,j}^{(i)} = \frac{\partial h}{\partial x}\left(\tilde{\mu}_{k,j}^{(i-1)}(c,m)\right) \tag{64}$$

$$P_{k,j}^{(i)}(c,m) = \left(I - K_{k,j}^{(i)} H_{k,j}^{(i)}\right) \tilde{P}_{k,j}^{(i-1)}(c,m) \tag{65}$$

$$K_{k,j}^{(i)} = \tilde{P}_{k,j}^{(i-1)}(c,m)\left(H_{k,j}^{(i)}\right)^{\mathsf{T}}\left(S_{k,j}^{(i)}\right)^{-1} \tag{66}$$

$$S_{k,j}^{(i)} = R^{(i)} + H_{k,j}^{(i)} \tilde{P}_{k,j}^{(i-1)}(c,m)\left(H_{k,j}^{(i)}\right)^{\mathsf{T}}. \tag{67}$$

Moreover, the likelihood function of class-based mode in (19) equals the normalization value of the class&mode-conditioned SPDF; thus, $\ell(m|c) = \Lambda^{(|\mathcal{N}|)}$ can be obtained by performing iterations until all sensors have been considered.

At the end of the above multi-sensor update procedure, the resulting posterior SPDFs $s_k(x|c, m)$ preserve the GM form with a number of GCs given by

$$J_k(c,m) = \left[\prod_{i\in\mathcal{N}} \left(|\mathcal{Z}_k^i| + 1\right)\right] J_{k|k-1}(c,m). \tag{68}$$

5.4 | Fusion of D-JDTC-BF

This subsection concerns the GM implementation of the fusion stage of D-JDTC-BF. For the sake of simplicity, we only consider pairwise fusion of two augmented Bernoulli densities $f^i = \{r^i, \gamma^i, \beta^i, s^i\}$, for $i = 1, 2$, with SPDFs in GM form,

$$s^i(x|c,m) = \sum_{j=1}^{J^i(c,m)} \alpha_j^i(c,m)\mathcal{G}\left(x;\mu_j^i(c,m),P_j^i(c,m)\right). \tag{69}$$

Unfortunately, the weighted geometric average of GMs

$$\tilde{s}(x|c,m) = \left[s^1(x|c,m)\right]^{\omega}\left[s^2(x|c,m)\right]^{1-\omega}, \tag{70}$$

due to exponentiation by the fractional exponents ω and $1-\omega$, is no longer a GM [33]. However, there exist reasonable approximations of Equation (70) in GM form such as, for example, Ref. [33]

$$\tilde{s}(x|c,m) \cong \sum_{j_1=1}^{J^1(c,m)}\sum_{j_2=1}^{J^2(c,m)} \alpha_{j_1,j_2}(c,m) \times \mathcal{G}\left(x;\mu_{j_1,j_2}(c,m),P_{j_1,j_2}(c,m)\right)$$

$$\alpha_{j_1,j_2}(c,m) = \left(\alpha_{j_1}^1\right)^{\omega}\left(\alpha_{j_2}^2\right)^{1-\omega}\varepsilon\left(\omega,P_{j_1}^1\right)\varepsilon\left(1-\omega,P_{j_2}^2\right) \times \mathcal{G}\left(\mu_{j_1}^1-\mu_{j_2}^2;0,\frac{P_{j_1}^1}{\omega}+\frac{P_{j_2}^2}{1-\omega}\right)$$

$$P_{j_1,j_2}(c,m) = \left[\omega\left(P_{j_1}^1\right)^{-1} + (1-\omega)\left(P_{j_2}^2\right)^{-1}\right]^{-1}$$

$$\mu_{j_1,j_2}(c,m) = P_{j_1,j_2}(c,m)\left[\omega\left(P_{j_1}^1\right)^{-1} + (1-\omega)\left(P_{j_2}^2\right)^{-1}\right]$$

$$\varepsilon(\omega,P) = \sqrt{\det(2\pi P\omega^{-1})\det(2\pi P)^{-\omega}}$$

where, for the sake of brevity, the arguments c and m of $\alpha_j^i, \mu_j^i, P_j^i$ have been omitted. An alternative approximation, more appropriate than Equation (71) whenever there are closely-spaced GCs, can be found in Ref. [37]. It is worth to point out that both approximations in Ref. [33, 37] produce a GM with a number of GCs given by

$$J(c,m) = J^1(c,m)J^2(c,m). \tag{71}$$

Then, according to Proposition 1, fused EP, MPMFs, CPMFs and SPDFs are obtained from Equations (22)–(25) by setting

$$\int \tilde{s}(x|c,m)dx = \sum_{j_1=1}^{J^1(c,m)}\sum_{j_2=1}^{J^2(c,m)} \alpha_{j_1,j_2}(c,m) \tag{72}$$

$$\tilde{r} = \left(r^1\right)^{\omega}\left(r^2\right)^{1-\omega} \tag{73}$$

$$\tilde{\gamma}(c) = \left[\gamma^1(c)\right]^{\omega}\left[\gamma^2(c)\right]^{1-\omega} \tag{74}$$

$$\tilde{\beta}(m|c) = \left[\beta^1(m|c)\right]^{\omega}\left[\beta^2(m|c)\right]^{1-\omega} \tag{75}$$

$$\tilde{\zeta} = \left(1-r^1\right)^{\omega}\left(1-r^2\right)^{1-\omega}. \tag{76}$$

Whenever fusion involves more than two sensor nodes, it is anyway possible to split it, in several ways, into a sequence of pairwise fusion steps to be performed as indicated above. Whatever is the adopted sequence, fusion over $\mathcal{N}$ of Proposition 1 generates GM SPDFs $\bar{s}(x|c,m)$ with

$$\bar{J}(c,m) = \prod_{i\in\mathcal{N}} J^i(c,m) \tag{77}$$

GCs, where $J^i(c, m)$ is the number of GCs of $s^i(x|c, m)$.

6 | SIMULATION RESULTS

Assume that the target can belong to three different classes with corresponding mode sets $\mathcal{M}_1 = \{m_1\}$, $\mathcal{M}_2 = \{m_1, m_2, m_3\}$ and $\mathcal{M}_3 = \{m_1, m_4, m_5\}$. The target kinematic state at time k is defined as $x_k = \left[\xi_k, \dot{\xi}_k, \eta_k, \dot{\eta}_k\right]^{\top}$, with Cartesian coordinates of position ξ_k, η_k and velocity $\dot{\xi}_k, \dot{\eta}_k$, respectively. For each kinematic mode, the target motion is modelled by (32) with

$$f(x,m) = F(m)x.$$

There are five possible modes and their corresponding state transition $F(m)$ and process noise covariance $Q(m)$ matrices are as follows:

Mode m_1:

$$F(m_1) = \begin{bmatrix} 1 & T & 0 & 0 \\ 0 & 1 & 0 & 0 \\ 0 & 0 & 1 & T \\ 0 & 0 & 0 & 1 \end{bmatrix}, \tag{78}$$

$$Q(m_1) = \sigma(m_1)\begin{bmatrix} \frac{2T^3}{3} & \frac{T^2}{2} & 0 & 0 \\ \frac{T^2}{2} & T & 0 & 0 \\ 0 & 0 & \frac{2T^3}{3} & \frac{T^2}{2} \\ 0 & 0 & \frac{T^2}{2} & T^2 \end{bmatrix}, \quad (79)$$

where $T = 1[s]$ denotes the sampling interval and $\sigma(m_1) = 1\ [m/s^2]$.

Mode m_2:

$$F(m_2) = \begin{bmatrix} 1 & \sin(\omega T)/\omega & 0 & (\cos(\omega T) - 1)/\omega \\ 0 & \cos(\omega T) & 0 & -\sin(\omega T) \\ 0 & (1 - \cos(\omega T))/\omega & 1 & \sin(\omega T)/\omega \\ 0 & \sin(\omega T) & 0 & \cos(\omega T) \end{bmatrix}, \quad (80)$$

$$Q(m_2) = \sigma(m_2)\begin{bmatrix} \frac{3T^4}{4} & \frac{T^3}{2} & 0 & 0 \\ \frac{T^3}{2} & T^2 & 0 & 0 \\ 0 & 0 & \frac{3T^4}{4} & \frac{T^3}{2} \\ 0 & 0 & \frac{T^3}{2} & T^2 \end{bmatrix} \quad (81)$$

where $\omega = -0.1[rad/s]$ and $\sigma(m_2) = 1.4[m/s^2]$.

Mode m_3: same as mode m_2 with $\omega = 0.15[rad/s]$ and $\sigma(m_3) = 1.4[m/s^2]$.

Mode m_4: same as mode m_2 with $\omega = 1[rad/s]$ and $\sigma(m_4) = 1.4[m/s^2]$.

Mode m_5: same as mode m_2 with $\omega = -1[rad/s]$ and $\sigma(m_5) = 1.4[m/s^2]$.

The transition probability matrices for classes 2 and 3 are

$$\Pi = \begin{bmatrix} 0.9 & 0.05 & 0.05 \\ 0.05 & 0.9 & 0.05 \\ 0.05 & 0.05 & 0.9 \end{bmatrix} \quad (82)$$

while class 1 has only one mode, that is, $\Pi = 1$.

The simulation duration is 100[s] for each experiment. The manoeuvring target, belonging to class 2, appears at time $t_a = 6$ [s] and disappears at $t_d = 90[s]$ in the surveillance region of angle extension $[0, \pi/2]$ [rad] and range extension $[0, 5000\sqrt{2}]$ [m]. The initial target state is,

$$x = [4786[m], -6.3[m/s], 3584[m], -60.9[m/s]]^\top. \quad (83)$$

Its trajectory (see Figure 2) is a straight line with constant velocity between 6[s] and 25[s], followed by a clockwise turn ($\omega = -0.10[rad/s]$) between 26[s] and 50[s], another straight line with constant velocity between 51[s] and 60[s], and a final counterclockwise turn ($\omega = 0.15[rad/s]$) between 61[s] and 90 [s]. Target modes over time are reported in Table 1.

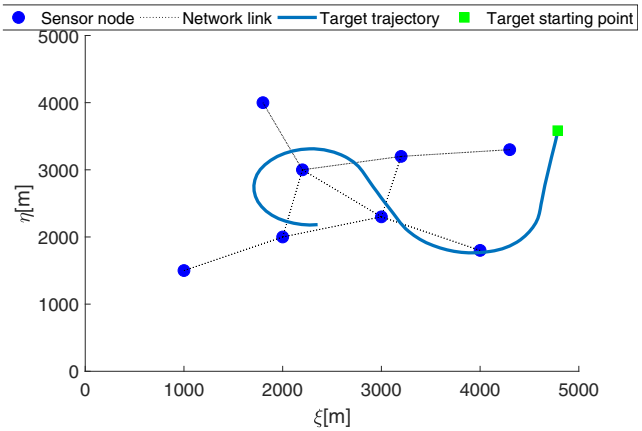

FIGURE 2 Sensor network and target track

A total of $|\mathcal{N}| = 8$ sensors are deployed over the surveillance area as shown in Figure 2. Each sensor $i \in \mathcal{N}$, of known position (ξ^i, η^i), provides a range measurement according to Equation (9) with the measurement function

$$h^i(x) = \sqrt{(\xi - \xi^i)^2 + (\eta - \eta^i)^2}, \quad (84)$$

and uniform detection probability $p_D^i = 0.90$ and measurement noise variance $R^i = 400[m^2]$. Clutter is generated as a Poisson RFS with PHD $\kappa(z) = \lambda u(z)$, with an expected number of clutter points $\lambda = 5$ and uniform spatial PDF $u(\cdot)$ over the surveillance region.

The JDTC-BF has been tuned with survival probability $p_S = 0.99$ and birth probability $p_B = 0.25$. Further, for target birth, we assumed uniform distribution for class and mode as well as class-and-mode independent Gaussian distribution for the state. Specifically, the target birth PDF has been taken as $b(x, c, m) = \gamma_B(c)\beta_B(m\,|\,c)s_B(x)$ with

$$\gamma_B(c) = \frac{1}{|\mathcal{C}|}$$
$$\beta_B(m|c) = \frac{1}{|\mathcal{M}_c|} \quad (85)$$
$$s_B(x) = \mathcal{G}(x; m_B, P_B)$$

where

$$m_B = [4780[m], -6[m/s], 3590[m], -60[m/s]]^\top,$$
$$P_B = \mathrm{diag}\left(\left[100\left[m^2\right], 100\left[m^2/s^2\right], 100\left[m^2\right], 100\left[m^2/s^2\right]\right]\right).$$

For D-JDTC-BF, the number of consensus steps has been set to $L = 1$. In particular, the pruning and merging thresholds for GMs are set to $T_p = 1 \times 10^{-15}$ and $T_m = 15$, respectively. Moreover, the maximum number of GCs is fixed to 3. For the

TABLE 1 Target modes and classes over time

Time	1–5 (s)	6–25 (s)	26–50 (s)	51–60 (s)	61–90 (s)	91–100 (s)
True mode	Disappearance	Mode 1	Mode 2	Mode 1	Mode 3	Disappearance
Possible class	Disappearance	Class 1, Class 2, and Class 3	Class 2	Class 1, Class 2, and Class 3	Class 2	Disappearance
True class	Disappearance	Class 2	Class 2	Class 2	Class 2	Disappearance

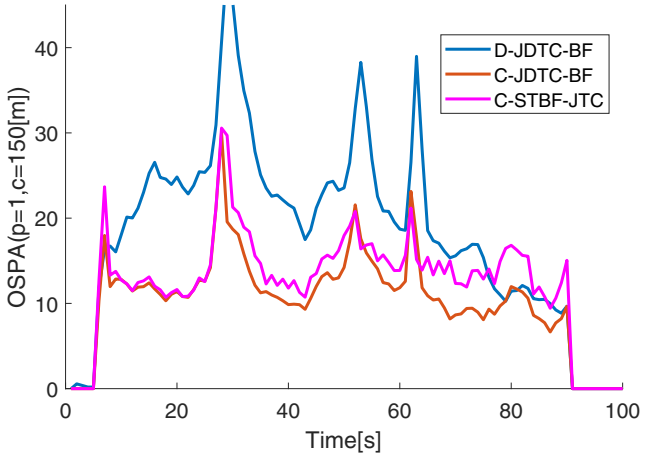

FIGURE 3 Optimal sub-pattern assignment error. BF, Bernoulli filter; C-JDTC, centralized JDTC; C-STBF-JTC, centralized joint tracking and classification via single-target Bayesian filtering; D-JDTC, distributed JDTC; JDTC, joint detection, tracking and classification

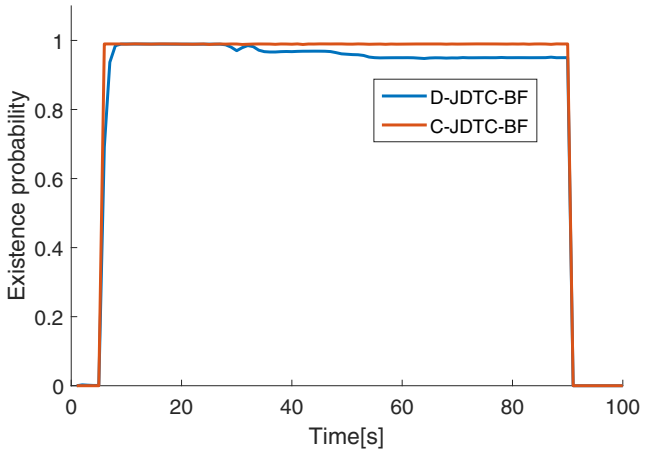

FIGURE 4 Existence probability. BF, Bernoulli filter; C-JDTC, centralized JDTC; D-JDTC, distributed JDTC; JDTC, joint detection, tracking and classification

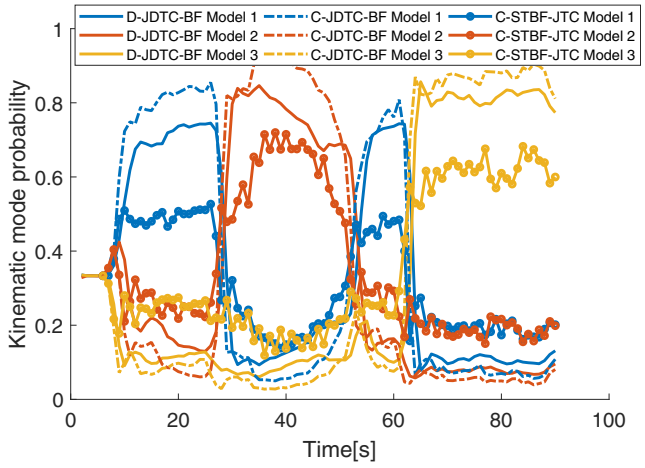

FIGURE 5 Mode probabilities for class 2. BF, Bernoulli filter; C-JDTC, centralized JDTC; C-STBF-JTC, centralized joint tracking and classification via single-target Bayesian filtering; D-JDTC, distributed JDTC; JDTC, joint detection, tracking and classification

sake of comparison, in the simulation experiments, also the centralized joint tracking and classification via single-target Bayesian filtering (C-STBF-JTC) is considered, in which the approach of Ref. [14] is applied in a centralized configuration by exploiting sequential single-sensor updates. Notice that no target detection is performed in this approach since exact knowledge of target existence/non-existence is assumed.

In the simulation experiments, performance will be evaluated in terms of four performance indicators averaged over 100 independent Monte Carlo trials: *optimal sub-pattern assignment* (OSPA) error [38] (with order $p = 1$ and cutoff $c = 150[m]$), existence probability, mode PMF, and classification probability.

The OSPA error is plotted in Figure 3, where it can be seen how the C-JDTC-BF clearly provides lower OSPA than the D-JDTC-BF and C-STBF-JTC as well as a smoother behaviour during class and/or mode switches. Specifically, all the three algorithms exhibit OSPA peaks after each class and/or mode switch: a first peak in the time interval 26–36 s is due to a simultaneous class and mode switch, while the subsequent two peaks (at time 53 and 63 s) are caused by mode switches.

As well known, the OSPA error simultaneously captures detection and tracking performance. A more clear-cut assessment of detection performance is provided by Figure 4, plotting the estimated existence probability. It can be seen that the detection capability of the D-JDTC-BF is close to that of the C-JDTC-BF (no results are reported for the C-STBF-JTC since this approach knows when the target appears/disappears).

Estimated mode PMFs for classes 2 and 3 versus time are plotted in Figures 5 and 6 (recall that class 1 has just a single mode). As expected, the C-JDTC-BF, D-JDTC-BF and C-STBF-JTC switch mode whenever the target turning rate changes. Since all three classes include mode 1, during the time interval 6–25 s mode 1 is estimated; then a switching to mode 2 occurs at time $t = 26$ s (see Figure 5).

Classification results are shown in Figure 7. First, as expected, the estimated class quickly converges to c_1 when the target appears in the monitored area. This is due to the transition probability of mode 1 in class 1 being greater than that

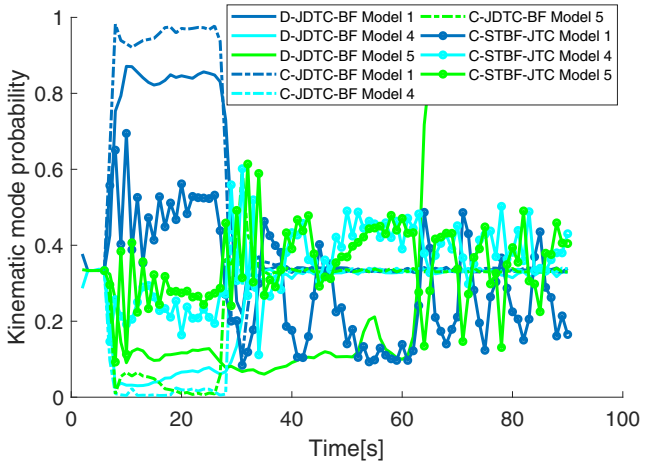

FIGURE 6 Mode probabilities for class 3. BF, Bernoulli filter; C-JDTC, centralized JDTC; C-STBF-JTC, centralized joint tracking and classification via single-target Bayesian filtering; D-JDTC, distributed JDTC; JDTC, joint detection, tracking and classification

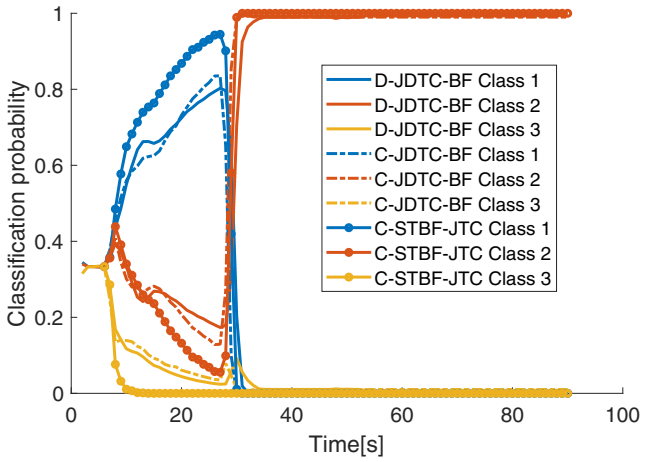

FIGURE 7 Classification results. BF, Bernoulli filter; C-JDTC, centralized JDTC; C-STBF-JTC, centralized joint tracking and classification via single-target Bayesian filtering; D-JDTC, distributed JDTC; JDTC, joint detection, tracking and classification

of mode 1 in class 2. At time $t = 26$ s, a switching from class 1 to class 2 occurs as soon as the target starts to behave according to mode 2. While the C-JDTC-BF and C-STBF-JTC exhibit faster class convergence than the D-JDTC-BF, after class switching a similar performance is observed. Furthermore, to compare the computational burden, the mean processing time is reported in Table 2 for all considered methods. Notice that the D-JDTC-BF involves a smaller per-node computational load compared to the one of the fusion centre for the C-JTDC-BF and C-STBF-JTC. Most importantly, the load of the distributed algorithm is scalable with respect to the network size while the one of the centralized algorithms would clearly increase with the number of sensors. The MATLAB code used in the simulations has been uploaded to GitHub (https://github.com/LGYbula/Matlab-code-for-multi-sensor-JDTC.).

TABLE 2 Computational load per time recursion

Algorithm	Time (s)
D-JDTC-BF	1.76 (per node)
C-JDTC-BF	2.88 (fusion centre)
C-STBF-JTC	2.61 (fusion centre)

Abbreviations: BF, Bernoulli filter; C-JDTC, centralized JDTC; C-STBF-JTC, centralized joint tracking and classification via single-target Bayesian filtering; D-JDTC, distributed JDTC; JDTC, joint detection, tracking and classification.

7 | CONCLUSION

JDTC of a single-target immersed in clutter has been addressed by multi-sensor fusion. The problem has been formulated in a Bayesian framework by introduction of a suitably augmented Bernoulli density describing the joint distribution of target class, mode and state. Then, the posed augmented *Bernoulli filtering* (BF) problem has been solved, in both centralized (C-JDTC-BF) and distributed (D-JDTC-BF) settings, and a Gaussian-mixture implementation of both filters has been presented. Simulation experiments have demonstrated the effectiveness of the proposed multi-sensor JDTC-BF approach. Future work will extend multi-sensor JDTC to multiple manoeuvring targets by exploiting *labelled multi-Bernoulli* (LMB) filtering. Moreover, we will further extend the multitarget JDTC problem to radar and ESM sensors [39–42] in airborne surveillance systems.

ACKNOWLEDGEMENTS

This work is supported by the National Natural Science Foundation of China under grant No. 62101112.

CONFLICT OF INTEREST

We state that none of the authors has any conflict of interest.

DATA AVAILABILITY STATEMENT

Research data are generated by a software code, which is made available on GitHub.

ORCID

Luigi Chisci https://orcid.org/0000-0001-5049-3577

REFERENCES

1. Farina, A., Studer, F.A.: Radar data processing: introduction and tracking. Research Studies Press Ltd. (1985)
2. Bar-Shalom, Y., Willett, P.K., Tian, X.: Tracking and data fusion: a handbook of algorithms. YBS Publishing (2011)
3. Yocom, B.A., et al.: A Bayesian approach to passive sonar detection and tracking in the presence of interferers. IEEE J. Ocean. Eng. 36(3), 386–405 (2011)
4. Petrovskaya, A., Thrun, S.: Model based vehicle detection and tracking for autonomous urban driving. Aut. Robots. 26(2), 123–139 (2009)
5. Robin, C., Lacroix, S.: Multi-robot target detection and tracking: taxonomy and survey. Aut. Robots. 40(4), 729–760 (2016)
6. Clarke, J.C., Zisserman, A.: Detection and tracking of independent motion. Image Vis Comput. 14(8), 565–572 (1996)
7. Vo, B.T., et al.: Multi-sensor joint detection and tracking with the Bernoulli filter. IEEE Trans. Aero. Electron. Syst. 48(2), 1385–1402 (2012)
8. Bar-Shalom, Y., Kirubarajan, T., Gokberk, C.: Tracking with classification-aided multiframe data association. IEEE Trans. Aero. Electron. Syst. 41(3), 868–878 (2005)

9. Benavoli, A., et al.: An approach to threat assessment based on evidential networks. In: 10th Int. Conf on Information Fusion (FUSION). Quebec, Canada, pp. 1–8 (2007)
10. Benavoli, A., et al.: An application of evidential networks to threat assessment. IEEE Trans. Aero. Electron. Syst. 45(2), 620–639 (2009)
11. Ristic, B., Smets, P.: Target classification approach based on the belief function theory. IEEE Trans. Aero. Electron. Syst. 41(2), 574–583 (2005)
12. Gordon, N.J., Maskell, S., Kirubarajan, T.: Efficient particle filters for joint tracking and classification. Int. J. Opt. Photonics. 4728, 439–449 (2002)
13. Challa, S., Pulford, G.W.: Joint target tracking and classification using radar and ESM sensors. IEEE Trans. Aero. Electron. Syst. 37(3), 1039–1055 (2001)
14. Yang, W., Fu, Y., Li, X.: Joint target tracking and classification via RFS-based multiple model filtering. Inf. Fusion. 18, 101–106 (2014)
15. Yang, W., et al.: Joint detection, tracking and classification of a manoeuvring target in the finite set statistics framework. IET Signal Process. 9(1), 10–20 (2015)
16. Yang, W., et al.: Joint detection, tracking and classification algorithm for multiple maneuvering targets based on LGJMS-GMPHDF. J. Electron. Inf. Technol. 34(2), 398–403 (2012)
17. Yang, W., Fu, Y.W., Li, X.: Joint detection, tracking and classification of multiple maneuvering targets based on the linear Gaussian jump Markov probability hypothesis density filter. Opt. Eng. 52(8), 083106 (2013)
18. Li, M., et al.: Multi-target joint detection, tracking and classification using generalized labeled multi-Bernoulli filter with Bayes risk. In: 19th Int. Conf on Information Fusion (FUSION). Heidelberg, Germany, pp. 680–687 (2016)
19. Gao, L., Sun, W., Wei, P.: Extensions of the CBMeMBer filter for joint detection, tracking, and classification of multiple maneuvering targets. Digit. Signal Process. 56, 35–42 (2016)
20. Yang, W., et al.: Joint detection, tracking, and classification of multiple targets in clutter using the PHD filter. IEEE Trans. Aero. Electron. Syst. 48(4), 3594–3609 (2012)
21. Javadi, S.H., Farina, A.: Radar networks: a review of features and challenges. Inf. Fusion. 61, 48–55 (2020)
22. Ilić, N., Stanković, M.S., Stanković, S.S.: Adaptive consensus-based distributed target tracking in sensor networks with limited sensing range. IEEE Trans. Control Syst. Technol. 22(2), 778–785 (2013)
23. Olfati-Saber, R., Sandell, N.F.: Distributed tracking in sensor networks with limited sensing range. In: American Control Conference. Seattle, Washington, USA, pp. 3157–3162 (2008)
24. Farina, A., Lombardo, P., Marsella, M.: Joint tracking and identification algorithms for multisensor data. IEE Proc. Radar, Sonar Navig. 149(6), 271–280 (2002)
25. Ristic, B., Farina, A.: Target tracking via multi-static Doppler shifts. IET Radar, Sonar Navig. 7(5), 508–516 (2013)
26. Guldogan, M.B.: Consensus Bernoulli filter for distributed detection and tracking using multi-static Doppler shifts. IEEE Signal Process. Lett. 21(6), 672–676 (2014)
27. Üney, M., Clark, D.E., Julier, S.J.: Distributed fusion of PHD filters via exponential mixture densities. IEEE J. Sel. Top. Signal Process. 7(3), 521–531 (2013)
28. Battistelli, G., et al.: Distributed fusion of multitarget densities and consensus PHD/CPHD filters. Int. J. Opt. Photonics. 9474, 94740E (2015)
29. Wang, B., et al.: Distributed fusion with multi-Bernoulli filter based on generalized covariance intersection. IEEE Trans. Signal Process. 65(1), 242–255 (2016)
30. Clark, D., et al.: Robust multi-object sensor fusion with unknown correlations. In: IET Sensor Signal Processing for Defence, p. 14 (2010)
31. Maher, R.P.: Statistical multisource-multitarget information fusion. Artech House (2007)
32. Mahler, R.P.: Optimal/robust distributed data fusion: a unified approach. Int. J. Opt. Photonics. 4052, 128–138 (2000)
33. Battistelli, G., et al.: Consensus CPHD filter for distributed multitarget tracking. IEEE J. Sel. Top. Signal Process. 7(3), 508–520 (2013)
34. Battistelli, G., et al.: Consensus-based multiple-model Bayesian filtering for distributed tracking. IET Radar, Sonar Navig. 9(4), 401–410 (2015)
35. Vo, B.T., Vo, B.N., Cantoni, A.: Analytic implementations of the cardinalized probability hypothesis density filter. IEEE Trans. Signal Process. 55(7), 3553–3567 (2007)
36. Vo, B.T., Vo, B.N., Cantoni, A.: The Gaussian mixture probability hypothesis density filter. IEEE Trans. Signal Process. 54(11), 4091–4104 (2006)
37. Vo, B.T., Vo, B.N., Cantoni, A.: Chernoff fusion of Gaussian mixtures based on sigma-point approximation. IEEE Trans. Aero. Electron. Syst. 52(6), 2732–2746 (2016)
38. Schuhmacher, D., Vo, B.T., Vo, B.N.: A consistent metric for performance evaluation of multi-object filters. IEEE Trans. Signal Process. 56(8), 3447–3457 (2008)
39. Farina, A., La Scala, B.: Methods for the association of active and passive tracks for airborne sensors. In: Int. Symposium on Radar, IRS98, Munich, Germany, pp. 735–744 (1998)
40. Farina, A., La Scala, B.: Effects of cross-covariance and resolution on track association. In: 3th Int. Conf on Information Fusion (FUSION). Sydney, NSW, Australia, pp. WED1–10 (2000)
41. La Scala, B.F., Farina, A.: Choosing a track association method. Inf. Fusion. 3(2), 119–133 (2002)
42. Farina, A., Miglioli, R.: Association of active and passive tracks for airborne sensors. Signal Process. 69(3), 209–217 (1998)

How to cite this article: Li, G., et al.: Distributed joint target detection, tracking and classification via Bernoulli filter. IET Radar Sonar Navig. 1–14 (2022). https://doi.org/10.1049/rsn2.12238

APPENDIX

Proof of Theorem 1

By substituting the augmented SPDF

$$s(x,c,m)=\gamma(c)\beta(m|c)s(x|c,m)$$

into Equation (21), we can obtain Equation (A.1).

Clearly, the fused augmented SPDF $\bar{s}(x,c,m)$ can be factored as the product of $\bar{\gamma}(c)$, $\bar{\beta}(m|c)$ and $\bar{s}(x|c,m)$, wherein $\bar{\gamma}(c)$, $\bar{\beta}(m|c)$ and $\bar{s}(x|m,c)$ are fused CPMF, MPMFs and SPDFs, respectively. Moreover, the fused EP is given by Equation (A.2),

where

$$\tilde{\zeta}=\prod_{i\in\mathcal{N}}\left(1-r^i\right)^{\omega^i}, \tag{A.3}$$

$$\tilde{r}=\prod_{i\in\mathcal{N}}\left(r^i\right)^{\omega^i}, \tag{A.4}$$

$$\tilde{\beta}(m|c)=\prod_{i\in\mathcal{N}}\left[\beta^i(m|c)\right]^{\omega^i}, \tag{A.5}$$

$$\tilde{\gamma}(c)=\prod_{i\in\mathcal{N}}\left[\gamma^i(c)\right]^{\omega^i} \tag{A.6}$$

$$\tilde{s}(x|c,m)=\prod_{i\in\mathcal{N}}\left[s^i(x|c,m)\right]^{\omega^i}dx. \tag{A.7}$$

$$
\begin{aligned}
\bar{s}(x,c,m) &= \frac{\prod_{i\in\mathcal{N}}\left[\gamma^i(c)\beta^i(m|c)s^i(x|c,m)\right]^{\omega^i}}{\sum_{c\in\mathcal{C}}\sum_{m\in\mathcal{M}_c}\int\prod_{i\in\mathcal{N}}\left[\gamma^i(c)\beta^i(m|c)s^i(x|c,m)\right]^{\omega^i}dx} \\
&= \frac{\prod_{i\in\mathcal{N}}\left[\gamma^i(c)\right]^{\omega^i}\left[\beta^i(m|c)\right]^{\omega^i}\left[s^i(x|c,m)\right]^{\omega^i}}{\sum_{c\in\mathcal{C}}\sum_{m\in\mathcal{M}_c}\int\prod_{i\in\mathcal{N}}\left[\gamma^i(c)\right]^{\omega^i}\left[\beta^i(m|c)\right]^{\omega^i}\left[s^i(x|c,m)\right]^{\omega^i}dx} \\
&= \frac{\prod_{i\in\mathcal{N}}\left[\gamma^i(c)\right]^{\omega^i}\prod_{i\in\mathcal{N}}\left[\beta^i(m|c)\right]^{\omega^i}\prod_{i\in\mathcal{N}}\left[s^i(x|c,m)\right]^{\omega^i}}{\sum_{c\in\mathcal{C}}\sum_{m\in\mathcal{M}_c}\prod_{i\in\mathcal{N}}\left[\gamma^i(c)\right]^{\omega^i}\prod_{i\in\mathcal{N}}\left[\beta^i(m|c)\right]^{\omega^i}\int\prod_{i\in\mathcal{N}}\left[s^i(x|c,m)\right]^{\omega^i}dx} \\
&= \frac{\prod_{i\in\mathcal{N}}\left[s^i(x|c,m)\right]^{\omega^i}}{\int\prod_{i\in\mathcal{N}}\left[s^i(x|c,m)\right]^{\omega^i}dx}\times\frac{\prod_{i\in\mathcal{N}}\left[\beta^i(m|c)\right]^{\omega^i}\int\prod_{i\in\mathcal{N}}\left[s^i(x|c,m)\right]^{\omega^i}dx}{\sum_{m\in\mathcal{M}_c}\left\{\prod_{i\in\mathcal{N}}\left[\beta^i(m|c)\right]^{\omega^i}\right\}\int\prod_{i\in\mathcal{N}}\left[s^i(x|c,m)\right]^{\omega^i}dx} \\
&\quad\times\frac{\prod_{i\in\mathcal{N}}\left[\gamma^i(c)\right]^{\omega^i}\sum_{m\in\mathcal{M}_c}\left\{\prod_{i\in\mathcal{N}}\left[\beta^i(m|c)\right]^{\omega^i}\right\}\int\prod_{i\in\mathcal{N}}\left[s^i(x|c,m)\right]^{\omega^i}dx}{\sum_{c\in\mathcal{C}}\left\{\prod_{i\in\mathcal{N}}\left[\gamma^i(c)\right]^{\omega^i}\right\}\sum_{m\in\mathcal{M}_c}\left\{\prod_{i\in\mathcal{N}}\left[\beta^i(m|c)\right]^{\omega^i}\right\}\int\prod_{i\in\mathcal{N}}\left[s^i(x|c,m)\right]^{\omega^i}dx} \\
&= \bar{s}(x|c,m)\bar{\beta}(m|c)\bar{\gamma}(c),
\end{aligned}
\tag{A.1}
$$

$$
\begin{aligned}
\bar{r} &= \frac{\prod_{i\in\mathcal{N}}\left(r^i\right)^{\omega^i}\sum_{c\in\mathcal{C}}\sum_{m\in\mathcal{M}_c}\int\prod_{i\in\mathcal{N}}\left[s^i(x|c,m)\beta^i(m|c)\gamma^i(c)\right]^{\omega^i}dx}{\prod_{i\in\mathcal{N}}\left(1-r^i\right)^{\omega^i}+\prod_{i\in\mathcal{N}}\left(r^i\right)^{\omega^i}\sum_{c\in\mathcal{C}}\sum_{m\in\mathcal{M}_c}\int\prod_{i\in\mathcal{N}}\left[s^i(x|c,m)\beta^i(m|c)\gamma^i(c)\right]^{\omega^i}dx} \\
&= \frac{\prod_{i\in\mathcal{N}}\left(r^i\right)^{\omega^i}\sum_{c\in\mathcal{C}}\left\{\prod_{i\in\mathcal{N}}\left[\gamma^i(c)\right]^{\omega^i}\right\}\sum_{m\in\mathcal{M}_c}\left\{\prod_{i\in\mathcal{N}}\left[\beta^i(m|c)\right]^{\omega^i}\right\}\int\prod_{i\in\mathcal{N}}\left[s^i(x|c,m)\right]^{\omega^i}dx}{\prod_{i\in\mathcal{N}}\left(1-r^i\right)^{\omega^i}+\prod_{i\in\mathcal{N}}\left(r^i\right)^{\omega^i}\sum_{c\in\mathcal{C}}\left\{\prod_{i\in\mathcal{N}}\left[\gamma^i(c)\right]^{\omega^i}\right\}\sum_{m\in\mathcal{M}_c}\left\{\prod_{i\in\mathcal{N}}\left[\beta^i(m|c)\right]^{\omega^i}\right\}\int\prod_{i\in\mathcal{N}}\left[s^i(x|c,m)\right]^{\omega^i}dx} \\
&= \frac{\tilde{r}\sum_{c\in\mathcal{C}}\tilde{\gamma}(c)\sum_{m\in\mathcal{M}_c}\tilde{\beta}(m|c)\int\tilde{s}(x|c,m)dx}{\tilde{\zeta}+\tilde{r}\sum_{c\in\mathcal{C}}\tilde{\gamma}(c)\sum_{m\in\mathcal{M}_c}\tilde{\beta}(m|c)\int\tilde{s}(x|c,m)dx},
\end{aligned}
\tag{A.2}
$$